Journal of Applied Polymer Science

Phototransparency and water vapor sorption properties of ABA-type triblock copolymers derived from 6FDA-TeMPD and poly(2-methyl-2-adamantylmethacrylate)

Shota Ando, Shimpei Konishi, Akihiro Yoshida, Kazukiyo Nagai
Department of Applied Chemistry, Meiji University, 1-1-1 Higashimita, Tama-Ku, Kawasaki 214-8571, Japan
Correspondence to: K. Nagai (E-mail: nagai@meiji.ac.jp or nagai@shikon.meiji.ac.jp)

ABSTRACT: The phototransparency and water vapor sorption properties of ABA-type triblock copolymer membranes derived from 4,4-(hexafluoroisopropylidene) diphthalic anhydride-2,3,5,6-tetramethyl-1,4-phenylenediamine (PI) and poly(2-methyl-2-adamantyl-methacrylate) (PMAdMA) were investigated, with focus on the effect of the adamantane component. The phototransparency of PMAdMA-*block*-PI-*block*-PMAdMA [Block(PI/PMAdMA)] was about 10–20% higher than that of poly(methyl methacrylate)-*block*-PI-*block*-Poly(methylmethacrylate) [Block(PI/PMMA)] because the high symmetric structure of adamantane inhibited photoabsorbance. The water vapor solubility of Block(PI/PMAdMA) decreased with increased PMAdMA because the PMAdMA had a hydrophobic property. Interestingly, in all relative-pressure regions, Block(PI/PMAdMA) with the least PMAdMA content showed a higher solubility coefficient than PI because the high mobility of PMAdMA in Block(PI/PMAdMA) resulted in additional sorption sites in the PI segment. A comparison of Block(PI/PMAdMA) with Block(PI/PMMA) in terms of relative pressure at the beginning of clustering further revealed that cluster formation in Block(PI/PMAdMA) was inhibited compared with Block(PI/PMMA) because bulky structure of adamantane restricted the mobility of the polymer main chain. © 2016 Wiley Periodicals, Inc. J. Appl. Polym. Sci. **2016**, *133*, 43795.

KEYWORDS: copolymers; functionalization of polymers; membranes; optical properties; swelling

Received 16 November 2015; accepted 15 April 2016
DOI: 10.1002/app.43795

INTRODUCTION

The development of flexible displays using plastic substrates is crucial for next-generation flat panel display such as liquid crystal displays and organic electronic luminescence. Transparent glass substrates must be replaced with transparent polymer membranes to reduce weight, make the membrane thinner, and increase shock resistance in flat panel displays. As alternative glass-substrate materials, polymer materials are required for high phototransparency, mechanical strength, processability, heat resistance, and gas-barrier properties from gas and water vapor in air.[1,2] Such barrier properties are important factors in various applications because device performance is strongly reduced by degradation even with a very small amount of gas or water vapor. Furthermore, water molecules cause the aging degradation and cloudiness of membrane because of the swelling and plasticization of polymer membrane structure resulting from the hydrogen bonding with water itself and the strong interaction with polymer.[3,4] Therefore, designing polymer materials is essential to reveal the interaction between a polymer segment and water vapor.[4]

Aromatic polyimides are widely used as electronic, optical, and display materials.[5–10] In particular, 4,4-(hexafluoro-isopropylidene) diphthalic anhydride-2,3,5,6-tetramethyl-1,4-phenylenediamine (PI) is preferred because of its high transparency, processability, excellent thermal stability, and mechanical strength. PI has lower coloration by charge-transfer (CT) complex than other polyimides because of its high free volume. However, result of water vapor sorption measurements have revealed the behavior of swelling and plasticization in PI with interaction of water molecules.[11] Thus, the degradation of phototransparency and mechanical strength of PI used for a long time in a humid atmosphere is of concern. In this study, we focused on the development of material that is compatible with phototransparency and is resistant to water vapor because these features are important in flexible-display applications. Our research group has previously reported that ABA-type triblock copolymer membranes derived from PI and poly(methyl methacrylate) (PMMA) have low water interaction, which effectively inhibits the influence of water vapor to membrane structures by water vapor sorption measurement.[11] However, the phototransparency of block copolymer was found to decrease compared with PI

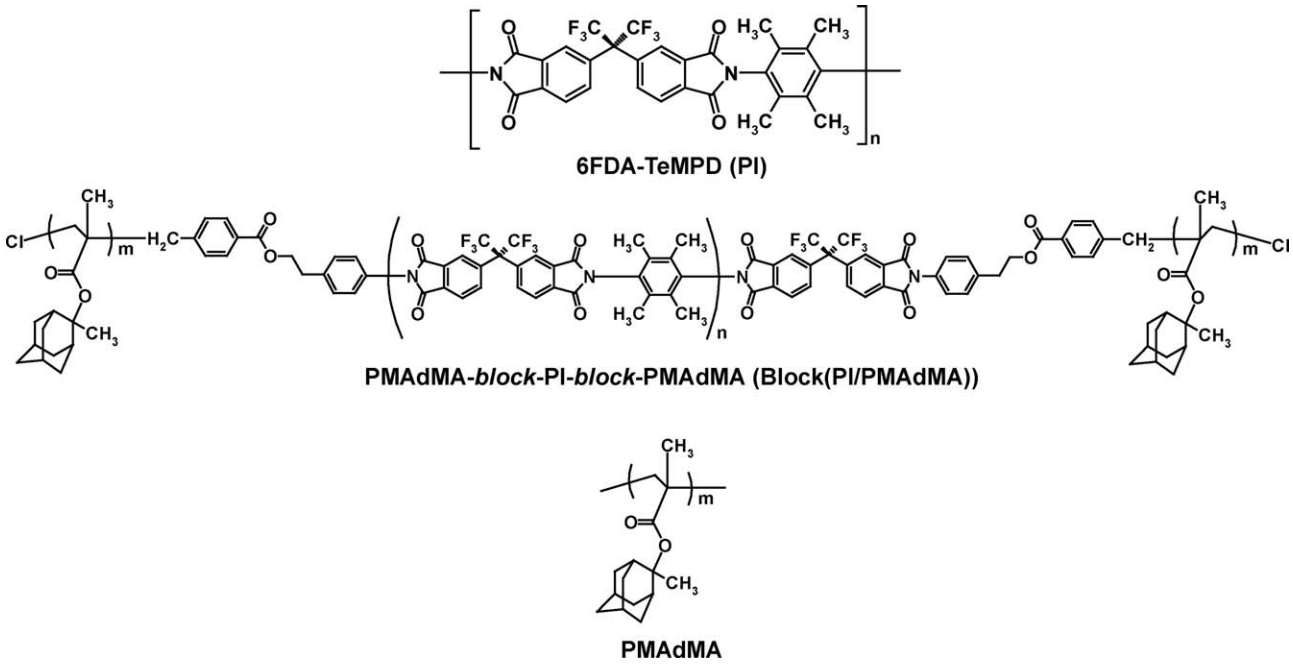

Figure 1. Chemical structure of PI, PMAdMA, and Block(PI/PMAdMA).

because of the formation of a phase-separation structure between two components by triblock copolymerization. Therefore, in the current work, we focused on ABA-type triblock copolymer derived from PI and 2-methyl-2-adamantylmethacrylate (2-MAdMA) as a solution of trade-off between phototransparency and water vapor interaction. 2-MAdMA is an adamantane-containing mathacrylate derivative, and adamantane is the smallest structure unit of diamond, which has a high symmetry and bulky structure. Given its structure, adamantane has high phototransparency and is colorless because of its narrow absorbent area of visible lights.[12–14] In addition, adamantane was reported by some study that enhances thermal stability[15–17] and gas permeability[17–20] of polymer because its bulky structure restricts the mobility of polymer chains. Moreover, 2-MAdMA was the best effectively inhibited the water vapor interaction in the homopolymer of methacrylate derivatives in previous study.[21]

In the present study, the phototransparency and water vapor sorption properties of [PMAdMA-*block*-PI-*block*-PMAdMA: Block(PI/PMAdMA)][2] membranes are systematically investigated in terms of the adamantyl group component by comparing PMMA-*block*-PI-*block*-PMMA [Block(PI/PMMA)] to the same Block(PI/PMAdMA) family, aiming to develop materials having high transparency and low water vapor interaction for flexible-display applications.

EXPERIMENTAL

Membrane Preparation

PI, PMAdMA, and triblock copolymers were used to synthesize a sample in the previous study.[22] The chemical structure of these polymers are shown in Figure 1.

Similar to a previous study,[22] the membranes in the present one were prepared on a poly(tetrafluoroethylene) Petri dish by casting 3 wt % chloroform solution to obtain a membrane thickness of 100–140 μm. The plate was covered with a glass dish to decrease the solvent evaporation rate and prevent contamination in atmospheric pressure at 23 ± 1 °C. The solvent in the membranes was allowed to evaporate for 72 h. The solvent was then removed by placing in a methanol solution at 23 ± 1 °C for 1 week. The membranes were dried at 100 °C for 12 h to remove the solvent. The PI and PMAdMA content rates in Block(PI/PMAdMA) were 61:39, 36:64, and 14:86 mol %, respectively, as calculated by ^{1}H-nuclear magnetic resonance. Afterward, Block(61/39), Block(36/64), and Block(14/86) were exhibited. The volume content rates of Block(PI/PMAdMA) were also 80:20, 57:43, and 28:72.

Characterization

All characterization data were obtained in membrane state using a minimum of three samples to confirm the reproducibility of experimental results.

The fractional free volume (*FFV*) of the polymers was determined using the following equation[23]:

$$FFV = \frac{V - 1.3V_w}{V} \quad (1)$$

where V is the polymer specific volume and V_w is the van der Waals volume calculated through the group contribution method of van Krevelen. The *FFV* of the copolymers was calculated based on the molar ratios of PI and PMAdMA.[24] The cohesive energy density (*CED*) was estimated using the group contribution method of van Kreveren.[23]

Ultraviolet-visible (UV-vis) spectra were obtained using a UV-3100 spectrophotometer (Shimadzu, Kyoto, Japan) at 23 ± 1 °C. The wavelength range was 200–800 nm.

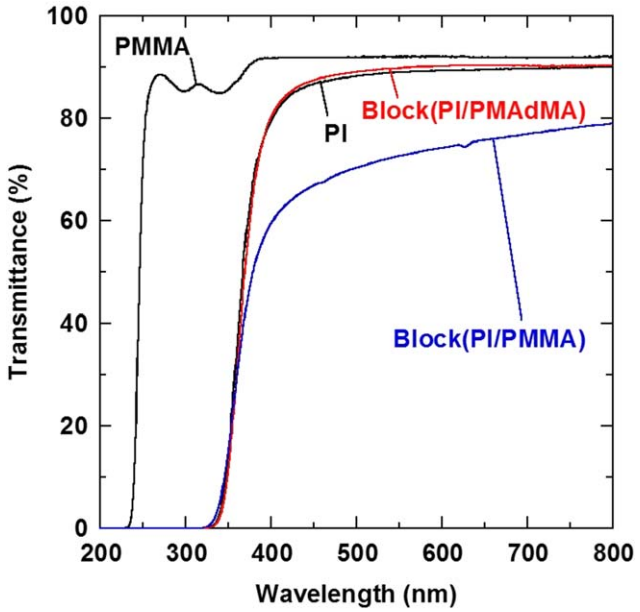

Figure 2. Ultraviolet-visible spectra of PI, PMMA, Block(PI/PMMA), and Block(PI/PMAdMA). [Color figure can be viewed in the online issue, which is available at wileyonlinelibrary.com.]

Water Vapor Sorption

The water vapor sorption in all the membranes was determined gravimetrically as a function of pressure at 35 °C using a calibrated helical quartz spring sorption system.[25] The sorption system was evacuated overnight at 35 °C after the sample was introduced into the chamber to degas the polymer membrane. Water vapor, which was removed completely by the dissolved gases through freeze drying, was introduced into the chamber at a fixed pressure. The resulting change in spring extension was monitored using differential transformer transducers and recorded up to 3.8 cmHg as a function of time. The saturated water vapor pressure (p_{sat}) at 35 °C was 4.23 cmHg.[26] The relative pressure (p/p_{sat}) of water vapor in the sorption experiments varied at a range of up to 0.8. The equilibrium of the sorbed water vapor concentration was calculated as follows[27]:

$$C = 22414 \times \frac{m_s \rho_p}{m_p M W_s} \quad (2)$$

where m_p is the polymer mass (g), m_s is the penetrant mass in the polymer (g), ρ_p is the polymer density (g/cm^3), MW_s is the penetrant molecular weight (g/mol), and 22,414 [cm^3(STP)/mol] is a conversion factor.

RESULTS AND DISCUSSION

Characterization

The UV-vis spectra of the Block(14/86) membranes are shown in Figure 2. For comparison, the results for PI, PMMA, and Block(PI/PMMA) (molar content rate of PI/PMMA:10/90) derived from PI and PMMA in our previous study are shown.[36] A flat membrane of 120 μm was obtained from Block(14/86), but was not obtained from Block(61/39), Block(36/64), and PMAdMA. Spectral data of adamantane- and nonadamantane-containing block copolymers showed that they possessed almost similar PI content rates. The transparency of Block(PI/PMMA) decreased by about 10–20% compared with that of PI and PMMA because of the formulation of microphase separation with PI and PMMA in Block(PI/PMMA).[2] In addition, the formulation of CT complex (CTC) was promoted through PMMA in Block(PI/PMMA). Kanehashi *et al.* also reported that PMMA block in Block(PI/PMMA) promoted the formulation of CTC in PI.[11] On the other hand, the transparency of Block(PI/PMAdMA) was almost similar to that of PI. Our previous fluorescence spectroscopy results showed that CT effect decreased with increased adamantane content rate. However, this trend was not observed between CT effect and molecular packing in Block(PI/PMAdMA). These results indicated that the symmetric structure of adamantane inhibited light absorbance in the membranes.

Water Vapor Sorption

For comparison, the water vapor sorption isotherms in each Block(PI/PMAdMA) and PI membranes at 35 °C with PMAdMA are presented in Figure 3. As shown in this figure, the dual-mode sorption model was well followed for these isotherms in all polymer membranes. The dual-mode sorption model is expressed by[28,29]

$$C = C_D + C_H = k_D p + \frac{C'_H b p}{1 + b p} \quad (3)$$

where C_D and C_H are the gas concentrations based on Henry's law sorption and Langmuir sorption, respectively. k_D is Henry's low coefficient and p is the gas pressure. b and C'_H are the Langmuir hole affinity parameter and capacity parameter, respectively. The dual-mode sorption model has been used to describe the solubility of gases in glassy polymers and in glassy, polar polymer as well. The concentration of the Block(PI/PMAdMA) membranes initially increased with increased water pressure following the dual-mode model; however, a significant upturn was observed at high pressure. The large degree of

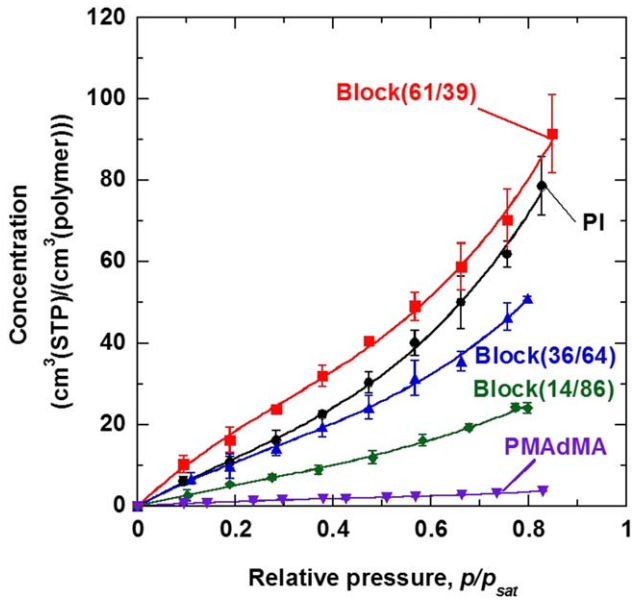

Figure 3. Water vapor sorption isotherms of Block(PI/PMAdMA) membranes at 35 °C. [Color figure can be viewed in the online issue, which is available at wileyonlinelibrary.com.]

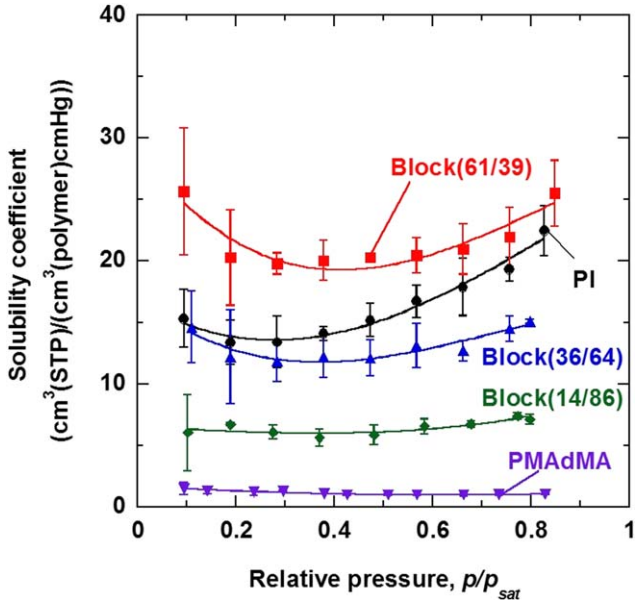

Figure 4. Water vapor solubility coefficients of Block(PI/PMAdMA) membranes as a function of water vapor relative pressure at 35 °C. [Color figure can be viewed in the online issue, which is available at wileyonlinelibrary.com.]

upturn at the high-pressure region may be attributed to the water molecules sorbed in the membranes, causing swelling and plasticization in the membranes, as well as clustering of water molecules.[4] The order of water concentration at the maximum pressure (i.e., $p/p_{sat} \approx 0.8$) was as follows: Block(61/39) > PI > Block(36/64) > Block(14/86) > PMAdMA. Water vapor concentration decreased with increased adamantane content because PMAdMA exhibited a hydrophobic property.[21] However, the water vapor concentration of Block(61/39) was higher than that of PI. The solubility of water vapor in polymer membranes can be expressed as follows:

$$S = \frac{C}{p} \tag{4}$$

where S is solubility coefficient {cm^3(STP)/[cm^3(polymer)cmHg]}, C is concentration {cm^3(STP)/[cm^3(polymer)]}, and p is vapor pressure (cmHg).

Figure 4 presents the solubility coefficient of water vapor in each polymer membrane as a function of relative pressure at 35 °C. With increased relative pressure, the solubility of all polymer membranes initially decreased based on the dual-mode model and then increased, indicating the clustering of water molecules with one another in the relative-pressure region between 0.3 and 0.6.

The water vapor solubility values at low ($p/p_{sat} < 0.1$), high pressures ($p/p_{sat} > 0.8$) and the infinite dilution solubility S_0 ($p/p_{sat} \approx 0$) can be determined by extrapolation are summarized in Table I. The order of solubility coefficients at low and high pressures was as follows: Block(61/39) > PI > Block(36/64) > Block(14/86) > PMAdMA. Interestingly, in all relative-pressure regions, Block(61/39) exhibited a higher solubility coefficient than PI. However, the solubility coefficient values of Block(61/39) were consistent with those of PI at high pressure ($p/p_{sat} > 0.7$). Based on the solubility data at low pressure (i.e., following the dual-mode model), Block(61/39) was hypothesized to have more nonexcess free volume, which can possibly dissolve water more than PI. By contrast, Block(61/39) had a lower interaction between the polymer segment and the water molecules than PI at high pressure, which was induced by membrane swelling and plasticization. These results suggested that adamantane caused resistance to plasticization through the interaction between the polymer segment and the water molecules. Furthermore, Paul *et al.* reported that hydrophilic polymer with high glass-transition temperature tended to increase the amount of sorption sites of water compared with hydrophilic polymer having a low glass-transition temperature.[30,31] Based on these results, the sorbed water in hydrophilic polyimide component and the effect of high mobility of methacrylate chain in the PMAdMA component tended to decrease the glass-transition temperature of Block(61/39). Therefore, in all the relative pressure regions, these effects provided several sorption sites of water in Block(61/39).

For comparison, Figures 5 and 6 present the relationship between water vapor solubility at low and high pressures in each polymer membranes as a function of *FFV* with some series of polymer-family membranes, such as polyimides,[32] polysulfones (PSF),[33] polyarylates (PA),[34] and adamantane-containing

Table I. Water Vapor Sorption Properties and Solubility Coefficient of Films

Polymer	PMAdMA content (vol %)	Sorption isotherm[a]	Solubility coefficient {cm^3(STP)/[cm^3(polymer)cmHg]} Low pressure (p/psat < 0.1)	High pressure (p/psat > 0.8)	Infinite dilution (a ≈ 0)	Relative pressure at clustering begins
PI	0	DMS + FH	15.32 ± 2.32	22.45 ± 2.04	15.99	0.33 ± 0.05
Block(61/39)	20	DMS + FH	25.64 ± 5.17	25.49 ± 2.69	28.19	0.48 ± 0.03
Block(36/64)	43	DMS + FH	14.63 ± 2.91	15.09 ± 0.16	16.15	0.43 ± 0.03
Block(14/86)	72	DMS + FH	6.03 ± 3.10	7.13 ± 0.37	8.02	0.66 ± 0.02
PMAdMA	100	DMS + FH	1.50 ± 0.49	1.04 ± 0.12	1.60	0.60 ± 0.01

[a] DMS, dual-mode sorption; FH, Flory-Huggins behavior.

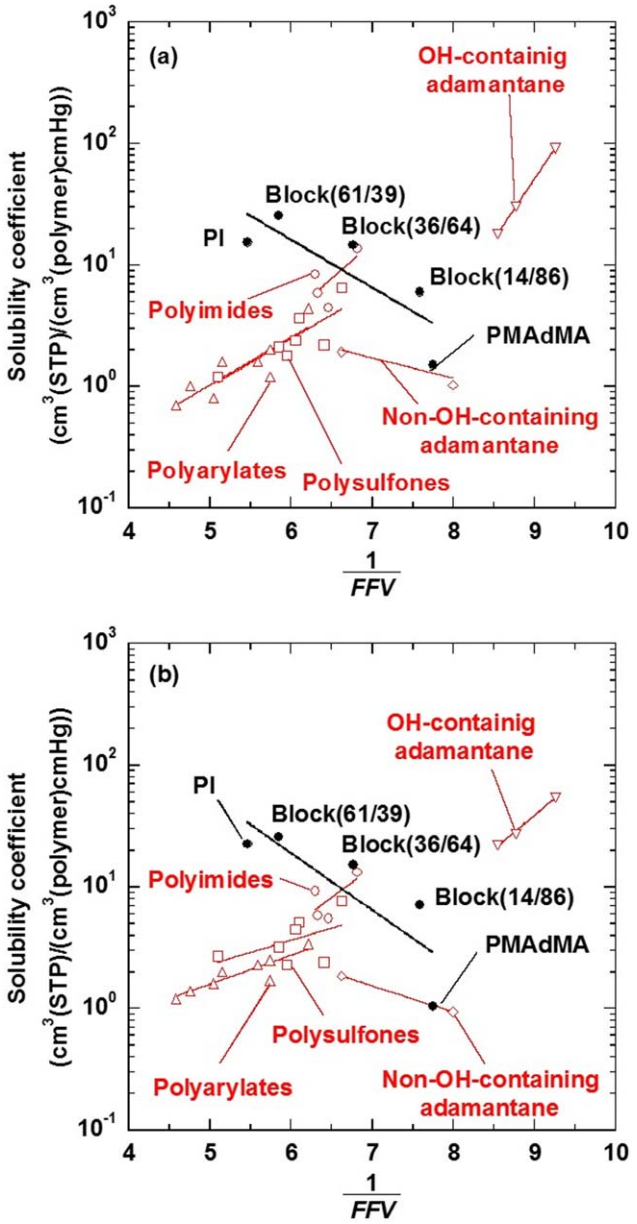

Figure 5. Water vapor solubility coefficients in Block(PI/PMAdMA) membranes as a function of the inverse of fractional free volume at 35 °C at (a) low relative pressure ($p/p_{sat} < 0.1$) and (b) high relative pressure ($p/p_{sat} > 0.8$). Polymers: Block(PI/PMAdMA) (●), polyimide (○), polysulfones (□), polyarylates (△), OH-containing adamantane (▽), and non-OH-containing adamantane (◇). [Color figure can be viewed in the online issue, which is available at wileyonlinelibrary.com.]

methacrylate polymers (Ad)[21] [Figure 5(a,b)], as well as composition polymer membranes, such as PSF + poly(vinyl pyrrolidone) (PVP),[31] polyethersulfone (PES)+polyethyloxazoline (PEOX),[30] and sulfonated polyimide (SUPI)[35] [Figure 6(a,b)]. Solubility at low and high pressures was given focus to investigate the effect of membrane swelling and plasticization. The polymer membranes were more stable at a lower region, whereas the membranes were more affected by the membrane swelling and plasticization induced by the sorbed water molecules at a higher region. Permanent gases (i.e., H_2, O_2, N_2, and CO_2) that did not strongly interact with the polymer generally showed increased solubility with increased free volume of polymer,[36,37] which can be expected theoretically.[30,31] PI, PSF, PA, OH-containing Ad, PSF + PVP, PES + PEOX, and SUPI exhibited an opposite trend at low and high pressures because the membrane structure changed (i.e., increased *FFV*), such as membrane swelling and plasticization. By contrast, Kanehashi *et al.* recently reported that a series of non-OH-containing Ad polymers family showed the same trend of solubility with

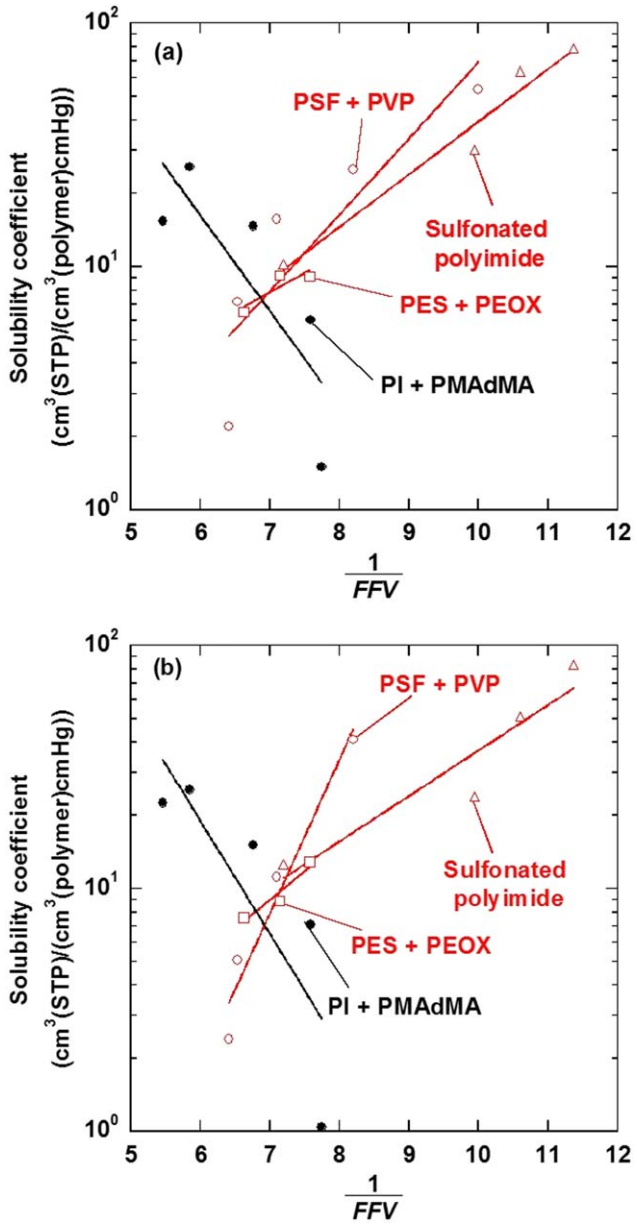

Figure 6. Water vapor solubility coefficients in Block(PI/PMAdMA) membranes as a function of the inverse of fractional free volume at 35°C at (a) low relative pressure ($p/p_{sat} < 0.1$) and (b) high relative pressure ($p/p_{sat} > 0.8$). Polymers: Block(PI/PMAdMA) (●), PSF + PVP (○), PES + PEOX(□), and sulfonated polyimide (△). [Color figure can be viewed in the online issue, which is available at wileyonlinelibrary.com.]

Table II. Parameters A_s and B_s in eq. (5)

Polymer	Temperature (°C)	A_s		B_s		Linear correlation coefficient (r^2)		Reference
		$p/p_{sat} < 0.1$	$p/p_{sat} > 0.8$	$p/p_{sat} < 0.1$	$p/p_{sat} > 0.8$	$p/p_{sat} < 0.1$	$p/p_{sat} > 0.8$	
Block(PI/PMAdMA)	35	9.49×10^{-3}	1.42×10^{-4}	-1.03	-1.10	0.794	0.783	This study
Polyimides	35	1.18×10^{-3}	4.86×10^{-3}	1.35	1.14	0.666	0.600	32
Polysulfones	40	0.0101	0.229	0.915	0.460	0.639	0.356	33
Polyarylates	40	0.0109	0.103	0.907	0.545	0.778	0.809	34
Adamantane Non-OH	35	25.3	49.7	-0.385	-0.497	0.827	0.999	21
Adamantane OH	35	6.30×10^{-8}	3.48×10^{-4}	2.28	1.29	0.999	0.996	21
PSF + PVP	40	0.0506	N/A	0.722	N/A	0.932	N/A	31
	40	N/A	3.05×10^{-4}	N/A	1.45	N/A	0.993	31
PES + PEOX	40	0.613	0.201	0.364	0.542	0.724	0.930	30
Sulfonated polyimide	20	0.268	0.496	0.499	0.431	0.943	0.905	35

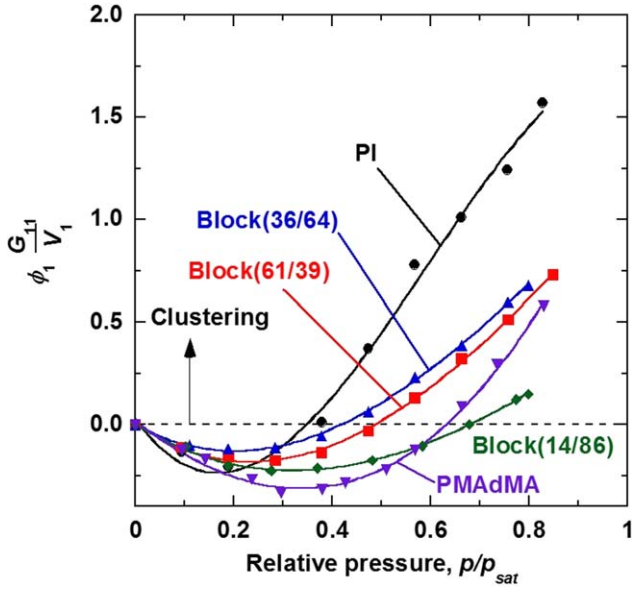

Figure 7. Cluster phenomenon in Block(PI/PMAdMA) membranes for water vapor at 35 °C as a function of water vapor relative pressure. [Color figure can be viewed in the online issue, which is available at wileyonlinelibrary.com.]

noncondensable gases because of the lower interaction between hydrophobic adamantane polymers and water molecules.[21] Block(PI/PMAdMA) also showed the same trend with non-OH-containing Ad polymers because of the effect of the hydrophobic PMAdMA component. PI, which was the main component of triblock copolymer, was hydrophilic with high free volume, whereas PMAdMA was more hydrophobic with low free volume compared with PI. This result indicated that increasing the adamantane component in Block(PI/PMAdMA) inhibited the increase in *FFV*, such as membrane swelling caused by sorbed

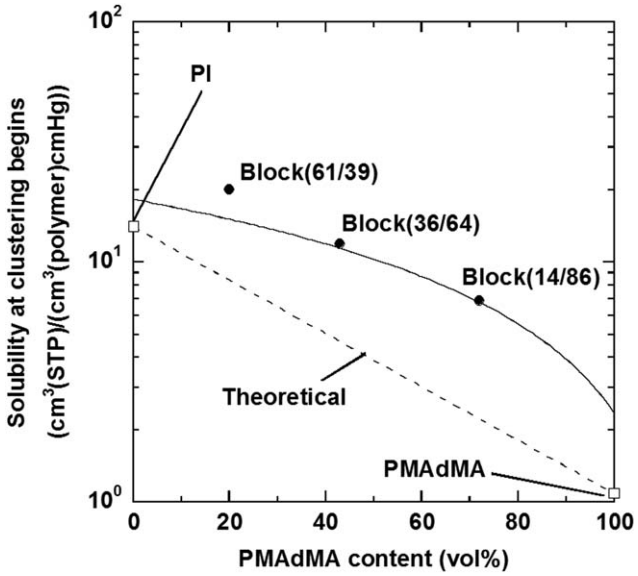

Figure 8. Water vapor solubility coefficient at the beginning of clustering in Block(PI/PMAdMA) membranes at 35 °C as a function of PMAdMA content.

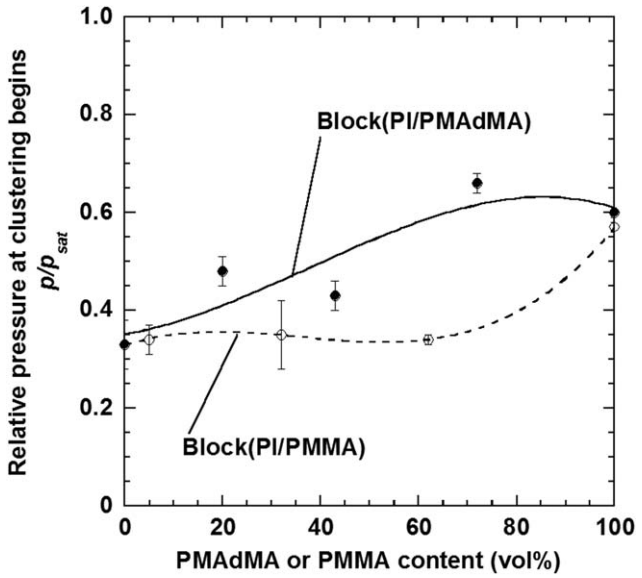

Figure 9. Relative pressure at the beginning of clustering in Block(PI/PMAdMA) and Block(PI/PMMA) membranes at 35 °C as a function of PMAdMA and PMMA content.

water. The data in Figures 5 and 6 were fitted in the following exponential function:

$$S = A_s exp\left(\frac{B_s}{FFV}\right) \quad (5)$$

where A_s and B_s are adjustable constants that depend only on the temperature and family of polymers. Based on the least-square fit analysis in Figures 5 and 6, A_s and B_s for each polymer in eq. (5) are summarized in Table II. An excellent correlation in Block(PI/PMAdMA) and in other families of polymers was observed. In this study, the composition of polymer membranes showed a higher linear correlation coefficient (r^2) than the series of polymer-family membranes. A_s tended to increase, whereas B_s decreased with increased relative pressure.

Water Vapor Clustering

Water molecule clusters formed through self-hydrogen bonding among OH groups. To investigate this clustering, the tendency of water molecules to cluster in polymer membranes was expressed in mathematical terms using the following Zimm–Lundberg formulation[38,39]:

$$\frac{G_{11}}{V_1} = -\phi_2\left[\frac{\partial(a_1/\phi_1)}{\partial a_1}\right]_{p,T} - 1 \quad (6)$$

where G_{11} is the cluster integral, V_1 is the partial molar volume of the water molecule, φ_1 and φ_2 are the volume fractions of the water molecule and polymer, respectively, and a_1 is the activity of water molecules. a_1 at a given activity can be determined from the equilibrium sorption isotherm using the following equation:

$$\phi_1 = \frac{\nu R}{1+\nu R'} \quad (7)$$

where ν is the ratio of the polymer density to water molecules, and R is the equilibrium sorption regained at $g_{(water)}/g_{(polymer)}$.

Figure 7 presents $\varphi_1 G_{11}/V_1$ determined from the water vapor sorption isotherm of triblock copolymers as a function of the water vapor relative pressure. Water molecules clustered in a certain relative pressure, suggesting that the value of $\varphi_1 G_{11}/V_1$ is positive (i.e., > 0). The relative pressure of triblock copolymers at the clustering point corresponded to $\varphi_1 G_{11}/V_1 = 0$, as summarized in Table I. When the value of $\varphi_1 G_{11}/V_1$ was negative (i.e., < 0), solubility was expressed based on the dual-mode sorption model at low pressure. The interaction between the polymer and the water molecules seemed larger than the interaction in the self-hydrogen bond among the water molecules at high relative pressure. The order of relative pressure at the clustering point was as follows: Block(14/86) > PMAdMA > Block(61/39) > Block(36/64) > PI.

Figure 8 presents the solubility at the clustering point in Block(PI/PMAdMA) as a function of adamantane content. In a series of adamantane-containing polymers, a linear water vapor solubility trend was observed at the cluster point and *CED*.[21] Therefore, the clustering of water molecules dissolved in the polymers was correlated with the molecular polarity of the polymers (i.e., *CED*). The *CED* value of the copolymer membrane changed according to the component ratio of each polymer, unless otherwise specified with the agglomeration of polymer chain, given that the *CED* value can be calculated from the chemical structure of polymer only. However, the experimental values of all the Block(PI/PMAdMA) in this study were higher than the theoretical line. This result indicated that the agglomeration of Block(PI/PMAdMA) was affected by an ABA-type structure. In particular, Block(61/39) had a higher concentration than PI because of the shorter adamantane block influence of polymer chain mobility. Therefore, copolymers with an ABA-type structure influenced polymer chain aggregation outside a structure change through polymer chain mobility.

Figure 9 presents the comparison between Block(PI/PMAdMA) and Block(PI/PMMA)[11] in terms of relative pressure at the beginning of clustering to analyze the inhibition effect by the adamantane. A cluster formed in the nonadamantane-containing Block(PI/PMMA) at almost the same relative pressure regardless of PMMA content. The order of relative pressure on each polymer is shown as follows; Block(14/86) > PMAdMA ≈ PMMA > Block(61/39) > Block(36/64) > PI ≈ Block(PI/PMMA). Meanwhile, the order of sorption concentration is shown as follows; Block(61/39) > PI > Block(36/64) > Block(14/86) > PMAdMA. It is reported that sorption of some glassy polymers on relative pressure at clustering begins is depended on sorption concentration. Thus, the order of Block(61/39) and Block(14/86) was specific result in this case. From these results, we considered effect of adamantan giving to PI. The Block(61/39) has shortest adamantane block in both side chain in Block(PI/PMAdMA)s. In the case, the short block has higher molecular mobility. Thus, it is considered that Langmuir site of terminal part of polyimide block. Therefore, relative pressure at clustering begin of Block(61/39) was increase because capacity of water molecules into the Langmuir site under low pressure region. On the other hands, Block(14/86) has longest adamantane block in both side chains in Block(PI/PMAdMA). In the case, effect of adamantane block was decrease to PI terminal

part because the long adamantane block has lower molecular mobility. Thus, Langmuir site was depended on adamantane content. Moreover, PI that has higher T_g than PMAdMA (PI: 424 °C,[40] PMAdMA: 141 °C[17]) restricted molecular mobility of adamantane block on one side chain. Therefore, relative pressure at clustering begin of Block(14/86) was higher than PMAdMA homopolymer.

CONCLUSIONS

The phototransparency and water vapor sorption properties of ABA-type triblock copolymer membranes derived from PI macroinitiator and PMAdMA were investigated, focusing on the effect of the adamantane component. The phototransparency of Block(PI/PMAdMA) was about 10–20% higher than that of Block(PI/PMMA) because adamantane with a high symmetric structure inhibited photoabsorbance in the membranes. The water vapor sorption measurement of Block(PI/PMAdMA) was determined at 35 °C. The solubility of Block(PI/PMAdMA) decreased with increased PMAdMA because PMAdMA exhibited a hydrophobic property. Interestingly, in all the relative-pressure regions, Block(61/39) showed a higher solubility coefficient than PI because the high mobility of PMAdMA in Block(PI/PMAdMA) resulted in additional sorption sites in the PI segment. Zimm–Lundberg analysis suggested that the cluster-inhibition effect in Block(PI/PMAdMA) was higher than that in PMAdMA. A comparison of Block(PI/PMAdMA) with Block(PI/PMMA) in terms of relative pressure at the beginning of clustering revealed that cluster formation in Block(PI/PMAdMA) was more inhibited than in Block(PI/PMMA) because adamantane with a bulky structure restricted the mobility of the polymer main chain and higher hydrophobicity derived from high symmetrical structure. Overall, results indicated that the adamantane structure had high symmetry, bulkiness, and hydrophobicity to polymer materials. Thus, adamantane has potential applications in areas that require phototransparency and water vapor resistance, such as electrical devices and packing materials.

ACKNOWLEDGMENTS

This research was partially supported by a Grant-in-aid for Scientific Research C (15K06493) from the Ministry of Education, Culture, Sports, Science and Technology, Japan, the Japanese Society of the Promotion of Science and Research Project Grant B (3) from the Institute of Science and Technology, Meiji University, Japan.

REFERENCES

1. Choi, M. C.; Kim, Y.; Ha, C. S. *Prog. Polym. Sci.* **2008**, *33*, 581.
2. Sato, S.; Ichikawa, M.; Ose, T.; Miyata, S.; Takahashi, Y.; Kanehashi, S.; Matsumoto, H.; Nagai, K. *Polym. Int.* **2013**, *62*, 1377.
3. Seo, J.; Han, H. *Polym. Degrad. Stabil.* **2002**, *77*, 477.
4. Paul, D. R. *Macromol. Symp.* **1999**, *138*, 13.
5. Yang, C. P.; Su, Y. Y. *Polymer* **2005**, *46*, 5797.
6. Creed, D.; Hoyle, C. E.; Subramanian, P.; Nagarajan, R.; Pandey, C.; Anzures, E. T.; Cane, K. M.; Cassidy, P. E. *Macromolecules* **1994**, *27*, 832.
7. Hoyle, C. E.; Anzures, E. T.; Subramanian, P.; Nagarajan, R.; Creed, D. *Macromolecules* **1992**, *25*, 6651.
8. Srisuwan, S.; Thongyai, S.; Praserthdam, P. *J. Appl. Polym. Sci.* **2010**, *117*, 2422.
9. Miyata, S.; Sato, S.; Nagai, K.; Nakagawa, T.; Kudo, K. *J. Appl. Polym. Sci.* **2008**, *107*, 3933.
10. Sato, S.; Ose, T.; Miyata, S.; Kanehashi, S.; Ito, H.; Matsumoto, S.; Iwai, Y.; Matsumoto, H.; Nagai, K. *J. Appl. Polym. Sci.* **2011**, *121*, 2794.
11. Kanehashi, S.; Koyama, Y.; Ando, S.; Konishi, S.; Shindo, R.; Miyata, S.; Sato, S.; Miyakoshi, T.; Nagai, K. *Polym. Int.* **2014**, *63*, 435.
12. Hsiao, S. H.; Li, C. T. *J. Polym. Sci. Part A: Polym. Chem.* **1999**, *37*, 1435.
13. Maehara, T.; Takenaka, J.; Tanaka, K.; Yamaguchi, M.; Yamamoto, H.; Ohshita, J. *J. Appl. Polym. Sci.* **2009**, *112*, 496.
14. Hattori, Y.; Miyajima, T.; Sakai, M.; Nagase, Y.; Nemoto, N. *Polymer* **2008**, *49*, 2825.
15. Matsumoto, A.; Tanaka, S.; Otsu, T. *Macromolecules* **1991**, *24*, 4017.
16. Acar, H. Y.; Jensen, J. J.; Thigpen, K.; McGowen, J. A.; Mathias, L. *J. Macromol.* **2000**, *33*, 3855.
17. Ando, S.; Yoshida, A.; Nakagawa, M.; Nagai, K. *J. Appl. Polym. Sci.* **2016**, submitted.
18. Maya, E. M.; Garcia-Yoldi, I.; Lozano, A. E.; de la Campa, J. G.; de Abajo, J. *Macromolecules* **2011**, *44*, 2780.
19. Bera, D.; Bandyopadhyay, P.; Ghosh, S.; Banerjee, S. *J. Membr. Sci.* **2014**, *453*, 175.
20. Chen, J.; Zhang, J.; Feng, Y.; Wu, J.; He, J.; Zhang, J. *J. Membr. Sci.* **2014**, *469*, 507.
21. Kanehashi, S.; Konishi, S.; Takeo, K.; Owa, K.; Kawakita, H.; Sato, S.; Miyakoshi, T.; Nagai, K. *J. Membr. Sci.* **2013**, *427*, 176.
22. Ando, S.; Koyama, Y.; Miyata, S.; Sato, S.; Kanehashi, S.; Nagai, K. *Polym. Int.* **2014**, *63*, 1634.
23. van Krevelen, D. W. Properties of Polymers, 4th ed.; Elsevier: Amsterdam, Netherlands, **2009**
24. Yeong, Y. F.; Wang, H.; Pallathadka Pramoda, K.; Chung, T. S. *J. Membr. Sci.* **2012**, *397–398*, 51.
25. Nagai, K.; Sugawara, A.; Kazama, S.; Freeman, B. D. *J. Polym. Sci. B: Polym. Phys.* **2004**, *42*, 2407.
26. Poling, B. E. The Properties of Gases and Liquids; McGraw-Hill: New York, United States, **2001**
27. Dixon-Garrett, S. V.; Nagai, K.; Freeman, B. D. *J. Polym. Sci. B: Polym. Phys.* **2000**, *38*, 1078.
28. Paul, D. R.; Yampol'skii, Y. P. Polymeric Gas Separation Membranes; CRC: Boca Raton, Florida, **1994**.
29. Kesting, R. E.; Fritzsche, A. K. Polymeric Gas Separation Membranes; John Wiley: New York, **1993**.

30. Schult, K. A.; Paul, D. R. *J. Polym. Sci. B: Polym. Phys.* **1997**, *35*, 993.
31. Schult, K. A.; Paul, D. R. *J. Polym. Sci. B: Polym. Phys.* **1997**, *35*, 655.
32. Lokhandwala, K. A.; Nadakatti, S. M.; Stern, S. A. *J. Polym. Sci. B: Polym. Phys.* **1995**, *33*, 965.
33. Schult, K. A.; Paul, D. R. *J. Polym. Sci. B: Polym. Phys.* **1996**, *34*, 2805.
34. Kelkar, A. J.; Paul, D. R. *J. Membr. Sci.* **2001**, *181*, 199.
35. Piroux, F.; Espuche, E.; Mercier, R.; Pineri, M. *J. Membr. Sci.* **2003**, *223*, 127.
36. Pixton, M. R.; Paul, D. R. *Polymer* **1995**, *36*, 3165.
37. Aitken, C. L.; Koros, W. J.; Paul, D. R. *Macromolecules* **1992**, *25*, 3424.
38. Lundberg, J. L. *Pure Appl. Chem.* **1972**, *31*, 261.
39. Zimm, B. H. *J. Chem. Phys.* **1953**, *21*, 934.
40. Shindo, R.; Kishida, M.; Sawa, H.; Kidesaki, T.; Sato, S.; Kanehashi, S.; Nagai, K. *J. Membr. Sci.* **2014**, *454*, 330.

SGML and CITI Use Only
DO NOT PRINT